Total Abdominal ^{18}F-FDG Uptake Reflects Intestinal Adenoma Burden in *Apc* Mutant Mice

Dianne M. Heijink[1,2], Jan H. Kleibeuker[2], Wouter B. Nagengast[1], Dorenda Oosterhuis[1], Adrienne H. Brouwers[3], Jan J. Koornstra[2], Steven de Jong[1], and Elisabeth G.E. de Vries[1]

[1]Department of Medical Oncology, University Medical Center Groningen, University of Groningen, Groningen, the Netherlands; [2]Department of Gastroenterology and Hepatology, University Medical Center Groningen, University of Groningen, Groningen, the Netherlands; and [3]Department of Nuclear Medicine, University Medical Center Groningen, University of Groningen, the Netherlands

Apc mutant (*Apc*^{Min}) mice develop multiple adenomas in their intestines and are widely used to study colorectal carcinogenesis and chemopreventive approaches. Molecular imaging of intestinal adenomas could potentially provide noninvasive longitudinal evaluation of these lesions in living mice. Therefore, the aim of this study was to investigate the role of ^{18}F-FDG PET in the *Apc*^{Min} mouse model. **Methods:** *Apc*^{Min} mice ($n = 8$) fed a purified diet were imaged serially after injection of ^{18}F-FDG at age 9 and 12 wk using a small-animal PET scanner. Abdominal uptake of the tracer was quantified. After dissection, intestines were imaged separately, and intestinal tracer uptake was quantified. Tracer distribution was compared with results from microscopic examination regarding adenoma number and size. Thereafter, findings were validated serially in 20 *Apc*^{Min} mice aged 6, 8, 10, and 12 wk that received standard chow to increase adenoma numbers. In vivo abdominal ^{18}F-FDG uptake was correlated with microscopy results. **Results:** Microscopic examination showed that the mice developed 25–35 intestinal adenomas at age 12 wk. Ex vivo ^{18}F-FDG PET of the dissected intestines visualized all large adenomas and most small adenomas. Ex vivo total intestinal ^{18}F-FDG uptake correlated with in vivo total abdominal uptake and with the number of large adenomas at age 9 and 12 wk. At 12 wk, there was a clear correlation between in vivo abdominal tracer uptake and the number of large adenomas but not the total number of lesions. **Conclusion:** Intestinal adenomas in *Apc*^{Min} mice are metabolically active lesions that take up ^{18}F-FDG. Abdominal ^{18}F-FDG uptake at age 12 wk serves as a readout modality for large intestinal adenomas.

Key Words: animal imaging; oncology; PET; *Apc*^{Min} mice; ^{18}F-FDG PET; colorectal adenomas

J Nucl Med 2011; 52:431–436
DOI: 10.2967/jnumed.110.083956

Colorectal cancer (CRC) develops from premalignant adenomas (*1*). Adenomas are common lesions with a prevalence at autopsy of around 35% in the Western world (*2*). Five percent of all colorectal adenomas will become malignant over a period of 5–10 y; thus, prevention of colorectal cancer is of substantial importance. The relatively slow evolution from normal mucosa to adenoma to cancer provides a window of opportunity for intervention. Chemoprevention involves the long-term use of agents to prevent, delay, or even reverse the development of adenomas and cancer, thereby interfering with the process of carcinogenesis (*3*). The most prominent candidates for chemoprevention, nonsteroidal anti-inflammatory drugs (NSAIDs), are effective but only in a subset of individuals. Current research, therefore, focuses on new, preferentially multitargeted approaches for chemoprevention (*4*).

In chemoprevention research, the *Apc* mutant (*Apc*^{Min}) mouse model is of interest because it mimics both familial adenomatous polyposis, a hereditary condition, and sporadic carcinogenesis. A truncating mutation in the *Apc* gene leads to multiple intestinal adenomas, especially located in the small intestine and to a lesser extent in the colon. These adenomas seldom progress toward malignancy, possibly because the mice die from anemia and cachexia before this transformation occurs (*5*). Despite the existing differences between colorectal carcinogenesis in humans and mice, most histologic and molecular features of adenomas in *Apc*^{Min} mice are similar to those observed in human adenomas (*6*). For this reason, and the fact that the heavy adenoma load facilitates the evaluation of chemopreventive effects, the *Apc*^{Min} mouse model is widely used for studying colorectal carcinogenesis and chemopreventive approaches.

Postmortem microscopic examination is the gold standard for assessing adenomas in the mouse intestine. This method does not allow continuous noninvasive monitoring of chemopreventive effects in the same mice over time. Using an effective longitudinal method to noninvasively follow intestinal adenoma development and growth in living mice could lead to better insight into treatment efficacy and could clearly lower the number of animals needed for those experiments. Noninvasive molecular imaging techniques, such as ^{18}F-FDG PET, which visualizes glucose metabolism, can potentially be of help in this respect. Malignant transformation is associated

Received Oct. 6, 2010; revision accepted Nov. 25, 2010.
For correspondence or reprints contact: Elisabeth G.E. de Vries, Department of Medical Oncology, University Medical Center Groningen, Hanzeplein 1, 9713 GZ Groningen, the Netherlands.
E-mail: e.g.e.de.vries@int.umcg.nl

with increasing glucose consumption. ^{18}F-FDG is actively taken up and accumulates in tumor cells (*7*). In humans, colorectal adenomas are detected by ^{18}F-FDG PET to a variable extent depending on adenoma characteristics (*8–19*). ^{18}F-FDG PET in a mouse model of intestinal adenomas has not been reported. The aim of this study was therefore to investigate the putative application of ^{18}F-FDG PET for the detection of intestinal adenomas in the *Apc*^{Min} mouse model, to evaluate its use for chemoprevention studies.

MATERIALS AND METHODS

Animals and Experimental Setup

Experimental protocols were approved by the Institutional Animal Care Committee. Heterozygous male C57BL/6J/*Apc*^{Min}/J mice (age, 5 wk) were obtained from Jackson Laboratories. Animals were housed in groups (4–5 mice) in a temperature-controlled room with a 12-h light–dark cycle and ad libitum food and water. Mice were put on a purified diet (AIN-93G; Dyets, Inc.) or fed standard chow to increase adenoma numbers (*20*). All animals received fresh food weekly. The mice (n = 4 per group) in the purified-diet group were scanned maximally twice at the ages of 9 and 12 wk. The mice (n = 5 per group) fed standard chow were scanned at 1, 2, 3, or maximally 4 times at the ages of 6, 8, 10, and 12 wk.

^{18}F-FDG PET

To improve ^{18}F-FDG adenoma uptake before scanning, mice were kept fasting overnight and allowed free access to water. Animals were kept warm starting from 30 min before tracer injection by keeping the cage temperature at 30°C using a heat lamp and a heating pad located beneath the cage (*21*). ^{18}F-FDG (15–20 MBq; pH 6.6–7.0; volume, <0.1 mL) was injected into the penile vein while mice were anesthetized (isoflurane anesthesia, induction, 3%, and maintenance, 1.5%). After tracer injection, mice were kept conscious, and warming continued during the uptake period of the tracer. PET was started at 60 min after ^{18}F-FDG injection, again under isoflurane anesthesia. Animals were imaged using a microPET Focus 220 rodent scanner (Siemens Preclinical Solutions, Inc.). Static images (acquisition time, 20 min) were obtained. Small-animal ^{18}F-FDG PET was performed in full 3-dimensional mode—that is, including oblique lines of response. Sinograms were Fourier rebinned into 2-dimensional sinograms and consecutively reconstructed using an attenuation-weighted ordered-subset expectation maximization iterative reconstruction. Data were corrected for randoms, scatter, attenuation, and dead time. The reconstructed scanner resolution was tested in phantom experiments and was 1.5 mm. After the last scan, animals were sacrificed directly by cervical dislocation, and the intestines were removed. Longitudinally opened intestines pinned on a paraffin layer were scanned after microscopic investigation, using the same scanning protocol. Decay correction was applied to enable comparison of ex vivo intestinal tracer uptake with whole-body data and with in vivo abdominal uptake in the living mice.

Calculation of Whole-Body, Abdominal, and Intestinal ^{18}F-FDG Uptake

Small-animal PET images were analyzed using AMIDE (A Medical Image Data Examiner) software (version 0.9.1; Stanford University). Whole-body activity (in MBq) was calculated by counting the total activity present within the image. For assessment of abdominal activity, a manually drawn volume of interest (VOI) in the abdomen was created (Fig. 1), and the total activity of this VOI was calculated. The VOI was constructed for each mouse separately, reaching from below the diaphragm. The bladder was left out of the VOI because ^{18}F-FDG is excreted in the urine, and bladder activity was prominently visible at 60 min after injection. Intestinal activity (in MBq) was assessed by calculating the total activity present in the ex vivo–scanned intestines. In vivo abdominal and ex vivo intestinal uptake were expressed as a percentage of whole-body uptake to correct for differences in injected tracer dose. Adenoma-to-background ratios were determined using the ex vivo images of the intestines of 9- and 12-wk-old mice. VOIs were constructed for adenoma regions and randomly chosen background regions of the small intestine. The maximum intensity of the adenoma and background VOIs was assessed (defined on a pixel basis). Ratios were calculated by dividing the maximum intensity of adenomas by the maximum intensity of the background.

Examination by Microscopy

The entire intestine from the pylorus to the rectum was removed and placed in ice-cold phosphate-buffered saline (PBS), pH 7.0. The intestine was divided into the following 4 segments (~4 cm each): proximal small intestine (duodenum), middle small intestine (jejunum), distal small intestine (ileum), and colon. Segments were opened longitudinally. Next, the intestines were rinsed with PBS and spread, using small pins on a paraffin layer in PBS, with the mucosal surface facing upward. Intestinal segments were examined under a dissecting microscope (Wild Heerbrugg) to record adenoma number, location, and diameter. Adenomas 2 mm or larger were classified as large adenomas in accordance with the literature (*22*). Schematic representations of the microscopic view were drawn to permit the comparison of microscopic results and results from ex vivo ^{18}F-FDG PET of the intestine.

Immunohistochemistry was performed on paraffin slides of the small intestine and colon of the mice using the following antibodies:

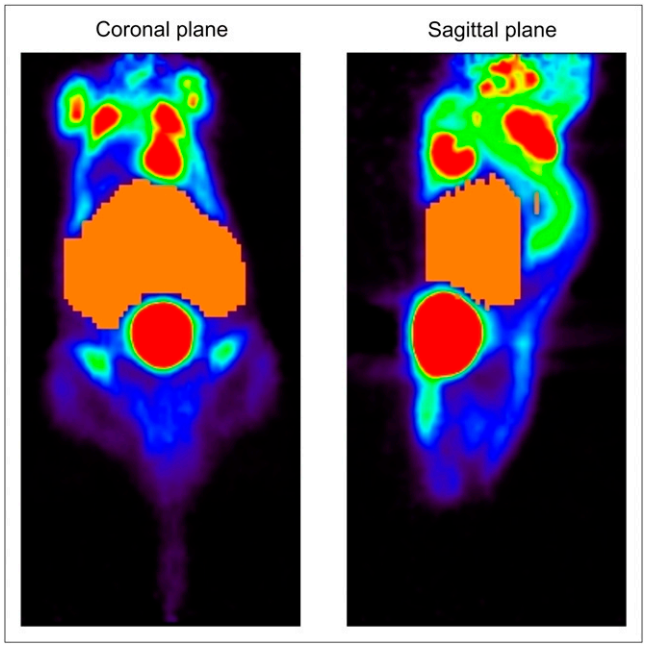

FIGURE 1. Whole-body ^{18}F-FDG PET images of *Apc*^{Min} mouse at age 12 wk. VOI to calculate abdominal uptake of tracer is shown in orange.

rat anti-Ki-67 (Dako) and rabbit anti–glucose transporter-1 (Chemicon International).

Statistical Analysis

SPSS (SPSS Inc.) for Windows (Microsoft) was used in all statistical analyses. The Mann–Whitney *U* test was used to determine differences in radioactivity uptake between groups. Linear regression analysis was used to determine the correlation between differently measured ^{18}F-FDG uptake percentages and between ^{18}F-FDG uptake and adenoma numbers. *P* values of less than 0.05 were considered statistically significant.

RESULTS

Adenoma Counts in *Apc*^{Min} Mice (Age, 9 and 12 Weeks)

Both the total number of adenomas and the number of adenomas 2 mm or larger as counted by microscopy did not differ between 9- and 12-wk-old mice (Table 1).

^{18}F-FDG PET Images in *Apc*^{Min} Mice (Age, 9 and 12 Weeks)

Visual analysis of the ^{18}F-FDG PET images showed several abdominal hot spots in each mouse, likely reflecting intestinal adenomas (Fig. 2A). It was unlikely that these hot spots represented physiologic uptake because liver and kidney uptake (in vivo imaging results) and normal small intestinal uptake (ex vivo imaging results) were relatively low, in line with published data (*23*). The number of hot spots did not correlate with the total number of adenomas or the number of large adenomas as counted by microscopy. When the intestines of the ^{18}F-FDG–injected mice were scanned ex vivo, all adenomas larger than 2 mm could be detected by ^{18}F-FDG PET in both 9- and 12-wk-old mice. Seventy-three percent and 97% of smaller adenomas were detected by ex vivo imaging of 9- and 12-wk-old mice, respectively (Fig. 2B). In addition, extra hot spots were found with ex vivo imaging in the small intestine of 9- (9%) and 12- (27%) wk-old mice in areas in which no adenoma was found at examination with the dissecting microscope. Although background uptake was relatively low in the small intestinal segments, the colon showed more ^{18}F-FDG uptake, and the degree of colonic background uptake strongly varied (1.3–3.7 times the background intensity of the small intestine). Immunohistochemistry for proliferation (Ki-67) and glucose transporter-1 revealed no differences in expression between small intestinal and colonic sections (data not shown).

TABLE 1
Adenoma Number in *Apc*^{Min} Mice (Age, 9 and 12 Weeks) Fed Purified Diet

Number of...	Age (wk) 9	Age (wk) 12	*P* (9 vs.12 wk)
Adenomas			0.39
Mean ± SD	26 ± 6.2	21.25 ± 8.2	
Range	19–33	12–30	
Adenomas ≥ 2 mm			0.81
Mean ± SD	6.25 ± 2.2	5.75 ± 2.2	
Range	4–11	3–8	

Abdominal and Intestinal Uptake of ^{18}F-FDG in *Apc*^{Min} Mice (Age, 9 and 12 Weeks)

Although the number of microscopically detected adenomas did not increase with age of the mice, the total uptake of ^{18}F-FDG in the ex vivo–scanned intestines did increase when expressed as a percentage of whole-body uptake ($P = 0.03$, Fig. 3A). The adenoma-to-background ratio was 1.4 for small and 2.1 for large (≥2 mm) adenomas at age 9 wk. At age 12 wk, the adenoma-to-background increased to 2.4 for small and 4.8 for large (≥2 mm) adenomas. These results demonstrate that ^{18}F-FDG was well distributed throughout the intestine and that adenomas are metabolically active lesions and take up ^{18}F-FDG to a higher extent than does normal small intestinal tissue. The uptake of ^{18}F-FDG in the total abdomen also increased with increasing age when expressed as a percentage of whole-body uptake ($P = 0.03$, $n = 4$ per group, Fig. 3B). The ex vivo intestinal tracer uptake at both age 9 wk and, especially, age 12 wk

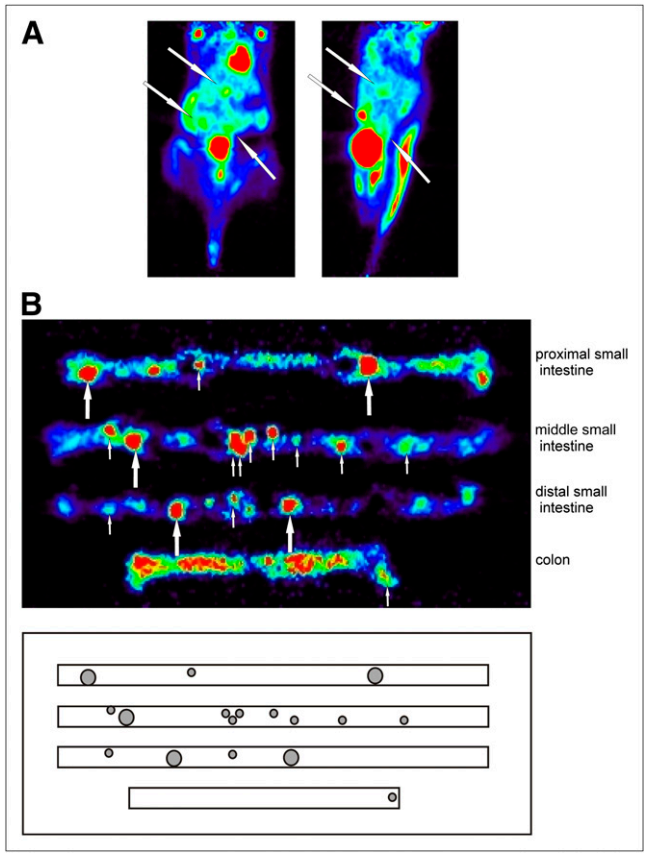

FIGURE 2. (A) Whole-body ^{18}F-FDG PET images of *Apc*^{Min} mouse at age 12 wk. Abdominal hot spots most likely reflecting intestinal adenomas are indicated by arrows. (B) ^{18}F-FDG PET of intestines of *Apc*^{Min} mouse at age 12 wk. Large arrows indicate large adenomas (≥2 mm), and small arrows indicate small adenomas (<2 mm). Schematic representation of microscopic view of intestine with adenomas is shown below ^{18}F-FDG PET image.

correlated with the in vivo abdominal uptake of the tracer (R^2 = 0.51 and 0.82, respectively; P = 0.28 and 0.09, respectively; n = 4 per group), indicating that the calculation of abdominal uptake can serve as a measure for intestinal uptake (Fig. 3C).

Correlation Between Intestinal Tracer Uptake and Microscopy

The ex vivo intestinal tracer uptake did not correlate with the total number of adenomas observed by microscopy (data not shown). However, ex vivo intestinal tracer uptake did correlate with the number of adenomas 2 mm or larger at age 9 and 12 wk (R^2 = 0.87 and 0.84, respectively; P = 0.07 and 0.08, respectively; n = 4 per group, Fig. 3D).

Correlation Between Abdominal Tracer Uptake and Microscopy

Because in vivo abdominal tracer uptake reflects ex vivo intestinal uptake of the tracer, we next assessed whether this abdominal uptake correlated with the number of adenomas 2 mm or larger. At the age of 12 wk, there was a clear correlation (R^2 = 1.0, P = 0.004, n = 4 per group, Fig. 4A), which did not exist at 9 wk of age (data not shown).

In a second larger cohort, we scanned and sacrificed mice at age 6, 8, 10, and 12 wk, to examine a larger time span and validate our previous results. To maximize the number of adenomas, these mice were fed standard chow, not a purified diet, because adenoma numbers are reportedly higher in standard chow–fed mice (*20*). At age 6 and 8 wk, an insufficient number of large adenomas (≥2 mm) was present for analysis (Table 2). In this cohort, there was again a correlation between in vivo abdominal tracer uptake and number of adenomas 2 mm or larger at age 12 wk (R^2 = 0.84, P = 0.03, n = 5 per group, Fig. 4B) but not at 10 wk (data not shown).

DISCUSSION

This study shows that intestinal adenomas in *Apc*^{Min} mice are metabolically active lesions that take up ^{18}F-FDG and that abdominal ^{18}F-FDG uptake at age 12 wk can serve as a readout modality for large intestinal adenomas.

In this study, adenomas could be visualized individually using ex vivo imaging of the intestines but not using in vivo imaging. Ex vivo stretching of the intestines minimizes fusion and overlay of hot spots due to the close proximity of adenomas, thus allowing visualization of individual lesions. In addition, less weakening and diversion occur in ex vivo imaging. Interestingly, when calculating the abdominal in vivo ^{18}F-FDG uptake, the sum of the uptake of ^{18}F-FDG in large adenomas detected adenoma-specific signals over background level. Therefore, ^{18}F-FDG PET

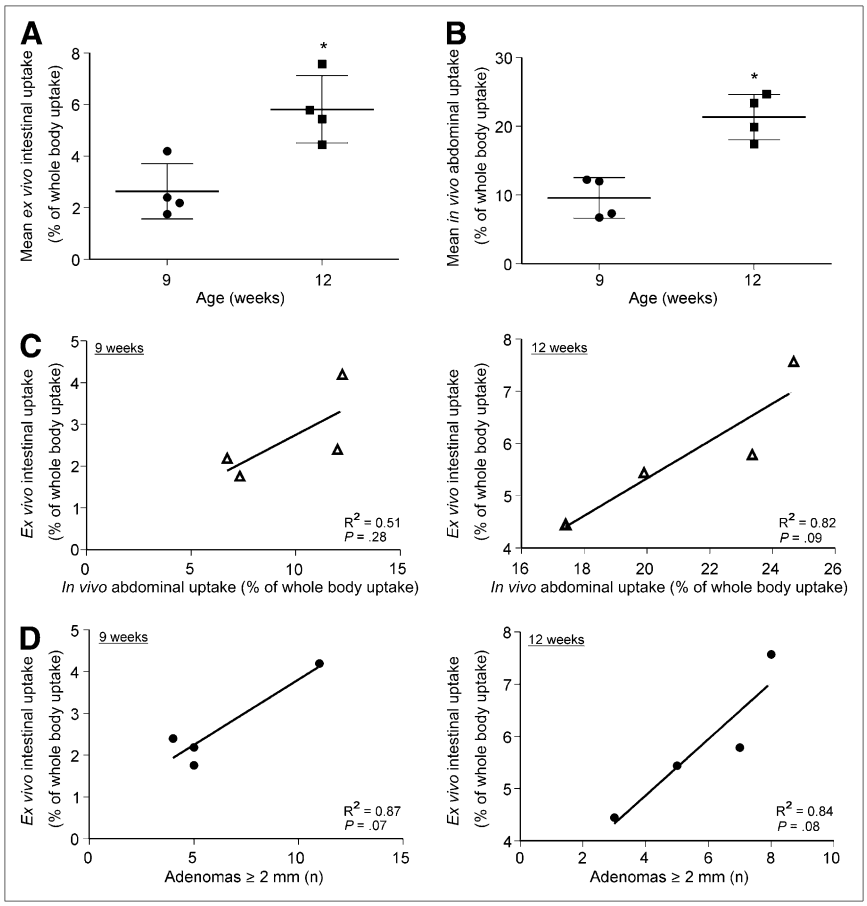

FIGURE 3. (A) Ex vivo intestinal ^{18}F-FDG uptake expressed as percentage of whole-body ^{18}F-FDG uptake in *Apc*^{Min} mice aged 9 (n = 4) and 12 (n = 4) wk. Mean and SD are displayed. (B) In vivo abdominal ^{18}F-FDG uptake expressed as percentage of whole-body ^{18}F-FDG uptake in *Apc*^{Min} mice aged 9 (n = 4) and 12 (n = 4) wk. Mean and SD are displayed. (C) Correlation between ex vivo intestinal ^{18}F-FDG uptake and in vivo abdominal ^{18}F-FDG uptake in 4 *Apc*^{Min} mice aged 9 wk and 4 *Apc*^{Min} mice aged 12 wk. (D) Correlation between ex vivo intestinal ^{18}F-FDG uptake and number of large intestinal adenomas based on microscopy in 4 *Apc*^{Min} mice aged 9 wk and 4 *Apc*^{Min} mice aged 12 wk. *P < 0.05.

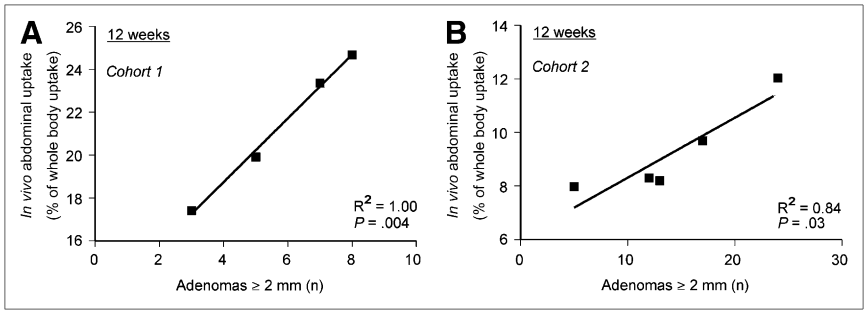

FIGURE 4. (A) Correlation between in vivo abdominal ^{18}F-FDG uptake and number of large intestinal adenomas in 4 *Apc*^{Min} mice aged 12 wk that were fed purified diet. (B) Correlation between in vivo abdominal ^{18}F-FDG uptake and number of large intestinal adenomas in 5 *Apc*^{Min} mice aged 12 wk that were fed standard chow.

seems especially suitable for follow-up studies in mice older than 8 wk because a sufficient number of large adenomas are present after this age. We observed a relationship between in vivo abdominal uptake and the number of large intestinal adenomas but not the total number of adenomas. This relationship may be first due to the fact that smaller aberrations are hard to detect in vivo because of partial-volume effects with a reconstructed scanner resolution of 1.5 mm, leading to decreased contrast and localization. Second, the degree of dysplasia may influence the detection. There are indications that the degree of dysplasia does indeed increase with the age of *Apc*^{Min} mice (*24,25*). The finding that the ex vivo intestinal ^{18}F-FDG uptake increased at age 12 wk, compared with at age 9 wk, whereas the number of (both total and large) adenomas did not, strengthens the hypothesis that more advanced dysplastic lesions were well detected by the small-animal PET scanner at age 12 wk. Possibly, adenoma numbers did not increase after age 9–10 wk because angiogenesis could not keep up with the fast-growing adenomas as a result of the chaotic microvasculature observed in 12-wk-old *Apc*^{Min} mice (*26*), leading to insufficient blood supply and stabilization or even regression of adenomas.

The relatively high background ^{18}F-FDG uptake in the colon, compared with the normal small intestine, could reflect differences in physiologic uptake between these 2 parts of the intestine in mice. ^{18}F-FDG uptake in the colon of humans has been related to smooth muscle activity and constipation (*27*). In addition, the increased colonic uptake could reflect a relatively high metabolic state caused by the *Apc* mutation. In morphologically normal colonic crypts of familial adenomatous polyposis patients with a proven *Apc* germline mutation, aberrant expression of proteins involved in, for example, transcription and mitosis was found (*28*). Thus, ^{18}F-FDG PET, compared with microscopic examination, could be even more sensitive because it provides information about glucose metabolism of the mouse intestine as a whole.

^{18}F-FDG PET to detect colorectal adenomas in humans has yielded variable results. When ^{18}F-FDG PET was compared with colonoscopy in patients with a suspected adenoma, colonoscopy was more sensitive than ^{18}F-FDG PET. The sensitivity of ^{18}F-FDG PET depended on the size of adenomas. Adenomas smaller than 0.5 cm were detected in 0%–33% of patients, whereas adenomas larger than 1 cm were detected in 59%–100% of patients (*8,11,12,17,18*). The degree of dysplasia also strongly influenced the detection capability of ^{18}F-FDG PET. Low-grade dysplastic adenomas were visualized in 13%–33% of patients, whereas high-grade adenomas were detected in 67%–76% of patients (*11,18*). In addition, 1 study reported that protruded adenomas were more easily detected than flat ones (*19*). In several studies, ^{18}F-FDG PET scans were retrospectively reviewed for abnormal colonic foci. If scan results were positive, a dysplastic adenoma was found in 32%–70% of patients by subsequent diagnostic colonoscopy, indicating that abnormal colonic hot spots at the ^{18}F-FDG PET scan frequently reflect adenomas (*10,15,16*). In rats, only 2 small studies have been performed assessing the role of ^{18}F-FDG PET in adenoma detection. In 1 study of 4 rats with a total of 2 adenomas (7 and 9 mm), both lesions were found with ^{18}F-FDG PET, although 1 of those lesions was found retrospectively (*29*). In a second study, the tumor-to-background ratio for 2 adenomas (<2 mm) in 19 rats was less than 1.0, indicating no higher tracer uptake in adenomas (*30*). Those experiments were, however, not conducted using an

TABLE 2
Adenoma Number in *Apc*^{Min} Mice (Age, 6, 8, 10, and 12 Weeks) Fed Standard Chow

Number of...	Age (wk)				*P* (10 vs. 12 wk)
	6	8	10	12	
Adenomas					0.02
Mean ± SD	19.2 ± 3.9	32 ± 9	59.6 ± 14.4	34.8 ± 10.8	
Range	19–23	23–41	44–82	17–46	
Adenomas ≥ 2 mm					0.96
Mean ± SD	0	1.3 ± 0.6	14 ± 5.0	14.2 ± 7	
Range	0	1–2	9–20	5–24	

animal scanner, which might have strongly negatively influenced the results because of a suboptimal resolution of the human scan system when used for small animals.

Besides ^{18}F-FDG PET, other imaging techniques could improve the visualization of colorectal adenomas in *Apc*^{Min} mice. CT isocontour analysis of ^{18}F-FDG PET was shown to be a sensitive method to identify preclinical, mild and severe inflammation in models of immune colitis in mice and could also detect treatment-induced alterations in inflammation (*31*). Micro-CT, compared with small-animal PET, provides a higher spatial resolution (0.3 mm). Combining micro-CT and small-animal PET might optimize visualization of colorectal adenomas. In addition, the precise effect of chemoprevention in a mouse model could be monitored via imaging of radiolabeled antibodies to a specific adenoma target—preferably already present in early-stage colorectal carcinogenesis, for example, COX-2, cyclin D1, or β-catenin.

CONCLUSION

Our study demonstrates the glucose metabolic activity of colorectal adenomas in *Apc*^{Min} mice. Molecular imaging using ^{18}F-FDG PET is suitable for visualizing the presence of colorectal adenomas in *Apc*^{Min} mice because abdominal ^{18}F-FDG uptake accurately reflects the number of large (≥2 mm) adenomas in the mouse intestine.

ACKNOWLEDGMENT

We thank Jurgen W.A. Sijbesma for excellent technical assistance. This study was supported by grant RUG 2005-3361 from the Dutch Cancer Society.

REFERENCES

1. Vogelstein B, Fearon ER, Hamilton SR, et al. Genetic alterations during colorectal-tumor development. *N Engl J Med.* 1988;319:525–532.
2. Nicum S, Midgley R, Kerr DJ. Colorectal cancer. *Acta Oncol.* 2003;42:263–275.
3. Arber N, Levin B. Chemoprevention of colorectal neoplasia: the potential for personalized medicine. *Gastroenterology.* 2008;134:1224–1237.
4. Ulrich CM, Bigler J, Potter JD. Non-steroidal anti-inflammatory drugs for cancer prevention: promise, perils and pharmacogenetics. *Nat Rev Cancer.* 2006;6:130–140.
5. McCart AE, Vickaryous NK, Silver A. Apc mice: models, modifiers and mutants. *Pathol Res Pract.* 2008;204:479–490.
6. Corpet DE, Pierre F. How good are rodent models of carcinogenesis in predicting efficacy in humans? A systematic review and meta-analysis of colon chemoprevention in rats, mice and men. *Eur J Cancer.* 2005;41:1911–1922.
7. Gambhir SS. Molecular imaging of cancer with positron emission tomography. *Nat Rev Cancer.* 2002;2:683–693.
8. Gollub MJ, Akhurst T, Markowitz AJ, et al. Combined CT colonography and ^{18}F-FDG PET of colon polyps: potential technique for selective detection of cancer and precancerous lesions. *AJR.* 2007;188:130–138.
9. van Kouwen MC, Drenth JP, van Krieken JH, et al. Ability of FDG-PET to detect all cancers in patients with familial adenomatous polyposis, and impact on clinical management. *Eur J Nucl Med Mol Imaging.* 2006;33:270–274.
10. Gutman F, Alberini JL, Wartski M, et al. Incidental colonic focal lesions detected by FDG PET/CT. *AJR.* 2005;185:495–500.
11. van Kouwen MC, Nagengast FM, Jansen JB, Oyen WJ, Drenth JP. 2-(^{18}F)-fluoro-2-deoxy-D-glucose positron emission tomography detects clinical relevant adenomas of the colon: a prospective study. *J Clin Oncol.* 2005;23:3713–3717.
12. Yasuda S, Fujii H, Nakahara T, et al. ^{18}F-FDG PET detection of colonic adenomas. *J Nucl Med.* 2001;42:989–992.
13. Drenth JP, Nagengast FM, Oyen WJ. Evaluation of (pre-)malignant colonic abnormalities: endoscopic validation of FDG-PET findings. *Eur J Nucl Med.* 2001;28:1766–1769.
14. Arslan N, Dehdashti F, Siegel BA. FDG uptake in colonic villous adenomas. *Ann Nucl Med.* 2005;19:331–334.
15. Israel O, Yefremov N, Bar-Shalom R, et al. PET/CT detection of unexpected gastrointestinal foci of ^{18}F-FDG uptake: incidence, localization patterns, and clinical significance. *J Nucl Med.* 2005;46:758–762.
16. Hemandas AK, Robson NK, Hickish T, Talbot RW. Colorectal tubulovillous adenomas identified on fluoro-2-deoxy-D-glucose positron emission tomography/computed tomography scans. *Colorectal Dis.* 2008;10:386–389.
17. Mainenti PP, Salvatore B, D'Antonio D, et al. PET/CT colonography in patients with colorectal polyps: a feasibility study. *Eur J Nucl Med Mol Imaging.* 2007;34:1594–1603.
18. Nakajo M, Jinnouchi S, Tashiro Y, et al. Effect of clinicopathologic factors on visibility of colorectal polyps with FDG PET. *AJR.* 2009;192:754–760.
19. Friedland S, Soetikno R, Carlisle M, Taur A, Kaltenbach T, Segall G. 18-Fluorodeoxyglucose positron emission tomography has limited sensitivity for colonic adenoma and early stage colon cancer. *Gastrointest Endosc.* 2005;61:395–400.
20. Beazer-Barclay Y, Levy DB, Moser AR, et al. Sulindac suppresses tumorigenesis in the Min mouse. *Carcinogenesis.* 1996;17:1757–1760.
21. Fueger BJ, Czernin J, Hildebrandt I, et al. Impact of animal handling on the results of ^{18}F-FDG PET studies in mice. *J Nucl Med.* 2006;47:999–1006.
22. Zhang L, Ren X, Alt E, et al. Chemoprevention of colorectal cancer by targeting APC-deficient cells for apoptosis. *Nature.* 2010;464:1058–1061.
23. Lee KH, Ko BH, Paik JY, et al. Effects of anesthetic agents and fasting duration on ^{18}F-FDG biodistribution and insulin levels in tumor-bearing mice. *J Nucl Med.* 2005;46:1531–1536.
24. Busquets L, Guillen H, DeFord ME, et al. Cathepsin E is a specific marker of dysplasia in APC mouse intestine. *Tumour Biol.* 2006;27:36–42.
25. Cooper HS, Everley L, Chang WC, et al. The role of mutant Apc in the development of dysplasia and cancer in the mouse model of dextran sulfate sodium-induced colitis. *Gastroenterology.* 2001;121:1407–1416.
26. Fuseler JW, Bedenbaugh A, Yekkala K, Baudino TA. Fractal and image analysis of the microvasculature in normal intestinal submucosa and intestinal polyps in Apc(Min/+) mice. *Microsc Microanal.* 2010;16:73–79.
27. Pandit-Taskar N, Schoder H, Gonen M, Larson SM, Yeung HW. Clinical significance of unexplained abnormal focal FDG uptake in the abdomen during whole-body PET. *AJR.* 2004;183:1143–1147.
28. Yeung AT, Patel BB, Li XM, et al. One-hit effects in cancer: altered proteome of morphologically normal colon crypts in familial adenomatous polyposis. *Cancer Res.* 2008;68:7579–7586.
29. Kuehle CA, Veit P, Antoch G, et al. Contrast-enhanced dark lumen PET/CT and MR colonography in a rodent polyp model: initial results with histopathologic correlation. *AJR.* 2005;185:1045–1047.
30. van Kouwen MC, Laverman P, van Krieken JH, Oyen WJ, Nagengast FM, Drenth JP. Noninvasive monitoring of colonic carcinogenesis: feasibility of [^{18}F]FDG-PET in the azoxymethane model. *Nucl Med Biol.* 2006;33:245–248.
31. Brewer S, McPherson M, Fujiwara D, et al. Molecular imaging of murine intestinal inflammation with 2-deoxy-2-[^{18}F]fluoro-D-glucose and positron emission tomography. *Gastroenterology.* 2008;135:744–755.